Perturbative QCD and factorization of coherent pion photoproduction on the deuteron

S. J. Brodsky
Stanford Linear Accelerator Center, Stanford University, Stanford, California 94309

J. R. Hiller
Department of Physics, University of Minnesota-Duluth, Duluth, Minnesota 55812

Chueng-Ryong Ji
Department of Physics, North Carolina State University, Raleigh, North Carolina 27695

G. A. Miller
Department of Physics, University of Washington, Seattle, Washington 98195

(Received 25 May 2001; published 18 October 2001)

We analyze the predictions of perturbative QCD for pion photoproduction on the deuteron $\gamma D\to\pi^0 D$ at large momentum transfer using the reduced amplitude formalism. The cluster decomposition of the deuteron wave function at small binding only allows the nuclear coherent process to proceed if each nucleon absorbs an equal fraction of the overall momentum transfer. Furthermore, each nucleon must scatter while remaining close to its mass shell. Thus the nuclear photoproduction amplitude $\mathcal{M}_{\gamma D\to\pi^0 D}(u,t)$ factorizes as a product of three factors: (1) the nucleon photoproduction amplitude $\mathcal{M}_{\gamma N_1\to\pi^0 N_1}(u/4,t/4)$ at half of the overall momentum transfer, (2) a nucleon form factor $F_{N_2}(t/4)$ at half the overall momentum transfer, and (3) the reduced deuteron form factor $f_d(t)$, which, according to perturbative QCD, has the same monopole falloff as a meson form factor. A comparison with the recent JLAB data for $\gamma D\to\pi^0 D$ of Meekins *et al.* [Phys. Rev. C **60**, 052201 (1999)] and the available $\gamma p\to\pi^0 p$ shows good agreement between the perturbative QCD prediction and experiment over a large range of momentum transfers and center-of-mass angles. The reduced amplitude prediction is consistent with the constituent counting rule $p_T^{11}\mathcal{M}_{\gamma D\to\pi^0 D}\to F(\theta_{\rm c.m.})$ at large momentum transfer. This is found to be consistent with measurements for photon lab energies $E_{\rm lab}>3$ GeV at $\theta_{\rm c.m.}=90°$ and $E_{\rm lab}>10$ GeV at 136°.

DOI: 10.1103/PhysRevC.64.055204 PACS number(s): 25.20.Lj, 24.85.+p, 13.60.Le, 12.38.Bx

I. INTRODUCTION

Most phenomena in nuclear physics can be well understood in terms of effective theories of dynamical nucleons and mesons. However, in some cases, conventional approaches to nuclear theory become inadequate, and the underlying quark and gluon degrees of freedom of nuclei become manifest. One such area where QCD makes testable predictions is exclusive nuclear processes involving high momentum transfer, such as the elastic lepton-nucleus form factors at large photon virtuality q^2, and scattering reactions such as deuteron photodisintegration $\gamma D\to pn$ and pion photoproduction $\gamma D\to\pi^0 D$ at large transverse momentum.

The predictions of QCD for nuclear reactions are most easily described in terms of light-cone (LC) wave functions defined at equal LC time $\tau=t+z/c$ [1]. The deuteron eigenstate can be projected on the complete set of baryon number $B=2$, isospin $I=0$, spin $J=1,J_z=0,\pm1$ color-singlet eigenstates of the free QCD Hamiltonian, beginning with the six-quark Fock states. Each Fock state is weighted by an amplitude that depends on the LC momentum fractions $x_i=k_i^+/p^+$ and on the relative transverse momenta $\boldsymbol{k}_{\perp i}$. There are five different linear combinations of six color-triplet quarks that make an overall color singlet, only one of which corresponds to the conventional proton and neutron three-quark clusters. Thus, the QCD decomposition includes four six-quark unconventional states with ''hidden color'' [2]. The spacelike form factors $F_{\lambda\lambda'}(Q^2)$ measured in elastic lepton-deuteron scattering for various initial and final deuteron helicities have exact representations as overlap integrals of the LC wave functions constructed in the Drell-Yan-West frame [3,4], where $q^+=0$ and $Q^2=-q^2=q_\perp^2$. At large momentum transfer, the leading-twist elastic deuteron form factors can be written in a factorized form

$$F_{\lambda\lambda'}(Q^2)=\int_0^1\prod_{i=1}^5 d_{x_i}\int_0^1\prod_{j=1}^5 d_{y_j}\phi_{\lambda'}(x_i,Q)\times T_H^{\lambda\lambda'}(x_i,y_i,Q)\phi_\lambda(y_j,Q),\qquad(1)$$

where the notation d_{x_i} indicates the integral is evaluated subject to the condition $\Sigma_i x_i=1$, the $\phi_\lambda(x_i,Q)$ are the deuteron distribution amplitudes, defined as the integral of the six-quark LC wave functions integrated in transverse momentum up to the factorization scale Q, and $T_H^{\lambda\lambda'}$ is the hard scattering amplitude for scattering six collinear quarks from the initial to final deuteron directions. A sum over the contributing color-singlet states is assumed. Because the photon and exchanged-gluon couplings conserve the quark chiralities and the distribution amplitudes project out $L_z=0$ components of initial and final wave functions, the dominant form factors at large momentum transfer are hadron-helicity conserving. The evolution equation for the distribution amplitudes is given in Refs. [2,5].

The hard-scattering amplitude scales as $(\alpha_s/Q^2)^5$ at leading order, corresponding to five gluons exchanged among the six propagating valence quarks. Higher order diagrams involving additional gluon exchanges and loops give next-to-leading order (NLO) corrections of higher order in α_s. Thus the nominal behavior of the helicity conserving deuteron form factors is $1/Q^{10}$, modulo the logarithmic corrections from the running of the QCD coupling and the anomalous dimensions from the evolution of distribution amplitudes. In fact, the measurement [6] of the high $Q^2 \geqslant 5$ GeV^2 helicity-conserving deuteron form factor $\sqrt{A(Q^2)}$ appears consistent with the $Q^{10}A(Q^2)$ scaling predicted by perturbative QCD and constituent counting rules [7].

The analogous factorization formulas for deuteron photodisintegration and pion photoproduction predict the nominal scaling laws $s^{11}d\sigma/dt(\gamma D \to np) \sim$ const and $s^{13}d\sigma/dt(\gamma D \to \pi^0 D) \sim$ const at high energies and fixed $\theta_{\rm c.m.}$. Comparison with the data shows this prediction is only successful at the largest momentum transfers [8–10]. This is not unexpected, since the presence of a large nuclear mass and a large number of partons involved can be expected to delay the onset of leading-twist scaling.

We may use an important simplifying feature of nuclear dynamics—the very weak binding of the deuteron state—to improve upon the above discussion. The cluster decomposition theorem [11] states that in the zero-binding limit $(B.E. \to 0)$, the LC wave function of the deuteron must reduce to a convolution of on-shell color-singlet nucleon wave functions,

$$\lim_{B.E.\to 0} \psi^D_{uududd}(x_i, \mathbf{k}_{\perp i}, \lambda_i) = \int_0^1 dz \int d^2 l_\perp \psi^d(z, l_\perp) \times \psi^p_{uud}(x_i/z, \mathbf{k}_{\perp i} + (x_i/z) l_\perp, \lambda_i) \times \psi^n_{udd}(x_i/(1-z), \mathbf{k}_{\perp i} - [x_i/(1-z)] l_\perp, \lambda_i), \tag{2}$$

where $\psi^d(z, l_\perp)$ is the reduced "body" LC wave function of the deuteron in terms of its nucleon components. Applying this cluster decomposition to an exclusive process involving the deuteron, one can derive a corresponding reduced nuclear amplitude (RNA) [5,12,13]. Moreover, at zero binding, one may take $\psi^d(z, l_\perp) \to \delta(z - m_p/(m_p + m_n))\delta^2(l_\perp)$. In effect, each nucleon carries half of the deuteron four-momentum. This approximation is very accurate, because the width of the deuteron momentum distribution is less than the square root of the ratio of the binding energy to the nucleon mass, ≈ 0.05. Furthermore, the deuteron wave function is vanishingly small for relevant values of the momentum transfer, which are of the order of a GeV. The deuteron does have Fock-space terms that are $NN\pi$ components, but the probability of these is very small, and they do not carry much momentum. There are $\Delta\Delta$ components, which have an even smaller probability, but might carry more momentum. We shall neglect such effects at the present time, choosing instead to examine less exotic possibilities. Similar observations can be made about hidden-color components in the deuteron wave function and other six-quark cluster components, which we also neglect. In short, our strategy here is to consider the most obvious effects first. The general dominance of the nucleonic part of the Fock space is caused by the very small binding energy of the deuteron. The other components enter with relatively large energy denominators.

Thus in the weak nuclear binding limit, the deuteron form factor reduces to the overlap of nucleon wave functions at half of the momentum transfer, and $F_D(Q^2) \to f_d(Q^2) F_N^2(Q^2/4)$ where the reduced form factor $f_d(Q^2)$ is computed from the overlap of the reduced deuteron wave functions [12]. The reduced deuteron form factor resembles that of a spin-one meson form factor since its nucleonic substructure has been factored out. Perturbative QCD predicts the nominal scaling $Q^2 f_d(Q^2) \sim$ const [5]. The measurements of the deuteron form factor show that this scaling is in fact well satisfied at spacelike $Q^2 \geqslant 1$ GeV^2 [6].

The reduced amplitude factorization is evident in the representative QCD diagram of Fig. 1. Half of the incident photon's momentum is carried over to the spectator nucleon by the exchanged gluon. The struck quark propagator is off shell with high virtuality $[x_1(p_D + q) + q/2]^2 \sim (1 + 2x_1)q^2/4 \sim q^2/3$ (using $x_1 \sim 1/6$) that provides the hard scale for the reduced form factor $f_d(Q^2)$. Figure 2 shows a similar diagram with quark interchange, which is consistent with the color-singlet clustered structure of the weak binding amplitude. Both of these diagrams become independent of the deuteron wave function when q is greater than about 1 GeV. In this case, one can represent the scattering amplitude as a product of two factors, one depending on the hard scattering and the other an integral of the deuteron wave function. The corrections to this factorization approximation are not computed here, but are estimated to be of order $1/P_T^2$.

In this work, we consider a similar analysis of pion photoproduction on the deuteron $\gamma D \to \pi^0 D$ at weak binding. The cluster decomposition of the deuteron wave function at small binding only allows this process to proceed if each nucleon absorbs an equal fraction of the overall momentum transfer. Furthermore, each nucleon must scatter while remaining close to its mass shell. Thus we expect the photoproduction amplitude to factor as

$$\mathcal{M}_{\gamma D \to \pi^0 D}(u,t) = C(u,t)\mathcal{M}_{\gamma N_1 \to \pi^0 N_1}(u/4, t/4) F_{N_2}(t/4). \tag{3}$$

Note that the on-shell condition requires the center-of-mass angle of pion photoproduction on the nucleon N_1 to be identical to the center-of-mass angle of pion photoproduction on the deuteron; the directions of incoming and outgoing particles in the nucleon subprocess must be the same as those of the deuteron process.

A representative QCD diagram illustrating the essential features of pion photoproduction on a deuteron is shown in Fig. 3. The exchanged gluon carries half of the momentum transfer to the spectator nucleon. Thus as in the case of the deuteron form factor the nuclear amplitude contains an extra quark propagator at an approximate virtuality $t/3$ in addition

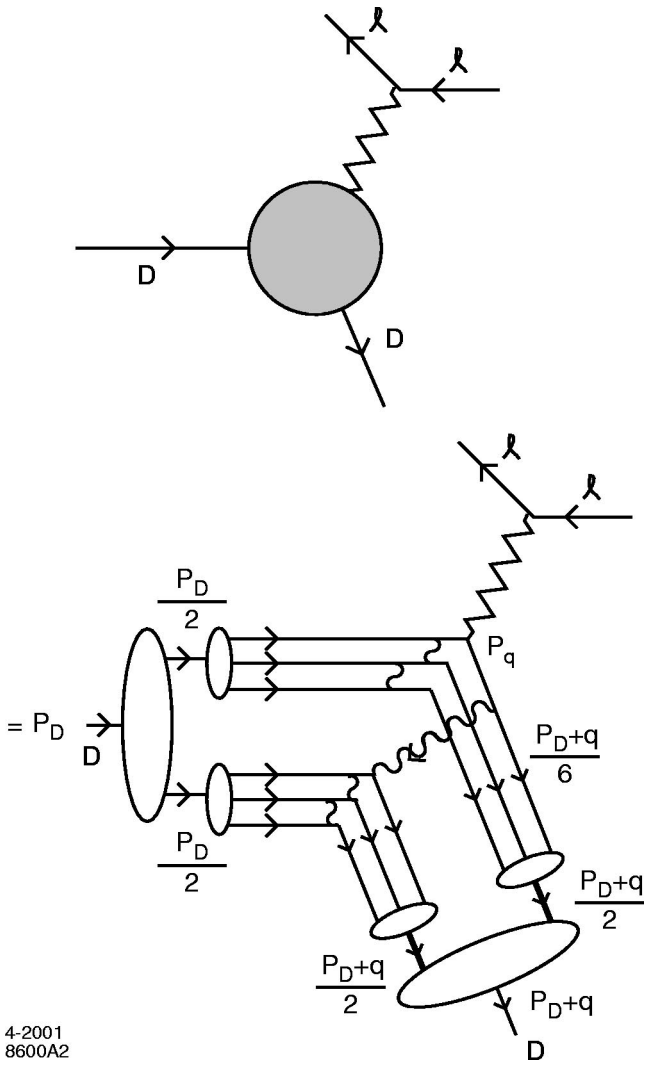

FIG. 1. Illustration of the basic QCD mechanism in which the nuclear amplitude for elastic electron deuteron scattering $lD \to lD$ factorizes as a product of two on-shell nucleon amplitudes. The propagator of the hard quark line labeled p_q is incorporated into the reduced form factor f_d.

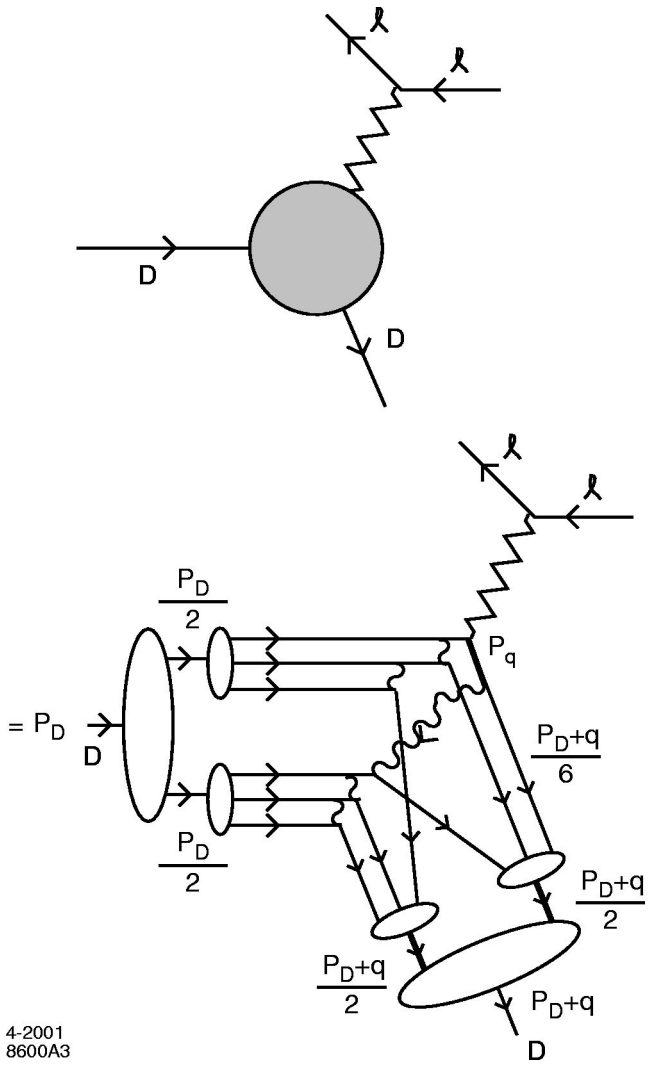

FIG. 2. Illustration of the basic QCD mechanism in which the nuclear amplitude for elastic electron deuteron scattering $lD \to lD$ factorizes as a product of two on-shell nucleon amplitudes. The quark interchange allows the amplitude to proceed when the deuteron wave function contains only color-singlet clusters.

to the on-shell nucleon amplitudes. Thus taking this graph as representative, we can identify $C(u,t) = C' f_d(t)$, where the constant C' is expected to be close to unity. This correspondence is also shown in Fig. 4 that includes a quark interchange to account for the color-singlet cluster structure. This structure predicts the reduced amplitude scaling

$$\mathcal{M}_{\gamma D \to \pi^0 D}(u,t) = C' f_d(t) \mathcal{M}_{\gamma N_1 \to \pi^0 N_1}(u/4, t/4) F_{N_2}(t/4). \tag{4}$$

A comparison with elastic electron scattering then yields the following proportionality of amplitude ratios,

$$\frac{\mathcal{M}_{\gamma D \to \pi^0 D}}{\mathcal{M}_{eD \to eD}} = C' \frac{\mathcal{M}_{\gamma p \to \pi^0 p}}{\mathcal{M}_{ep \to ep}}. \tag{5}$$

More details of the derivation for Eq. (4) will be presented in the following section. The normalization is fixed by the requirement that this factorization yields the same result as the full counting rules for $\mathcal{M}$ in the asymptotic limit. Fixing the normalization at a nonasymptotic energy can be a poor approximation, as can be seen in a recent analysis [14].

The new factored form, Eq. (4), differs significantly from the older reduced nuclear amplitude factorization [13], for which

$$\mathcal{M}^{\text{older}}_{\gamma D \to \pi^0 D}(u,t) \simeq m_{\gamma d \to \pi^0 d}(u,t) F_N^2(t/4). \tag{6}$$

Here $m_{\gamma d \to \pi^0 d}$ is the reduced amplitude; it scales the same as $m_{\gamma \rho \to \pi^0 \rho}$ at fixed angles since the nucleons of the reduced deuteron d are effectively pointlike. The advantages of this reduction are that some nonperturbative physics is included via the nucleon form factors and that systematic extension to many nuclear processes is possible [13]. The new factorization given by Eq. (4) is an improvement because it includes nonperturbative effects in the pion production process itself.

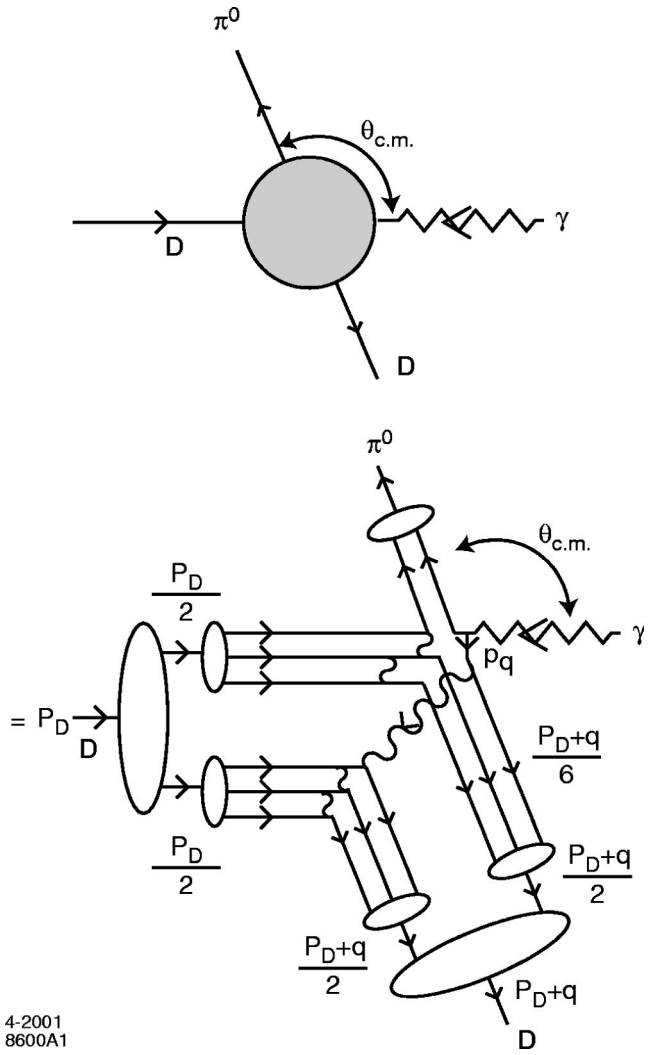

FIG. 3. Illustration of the basic QCD mechanism in which the nuclear amplitude for $\gamma D \to \pi^0 D$ factorizes as a product of two on-shell nucleon amplitudes. The propagator of the hard quark line labeled p_q is incorporated into the reduced form factor f_d.

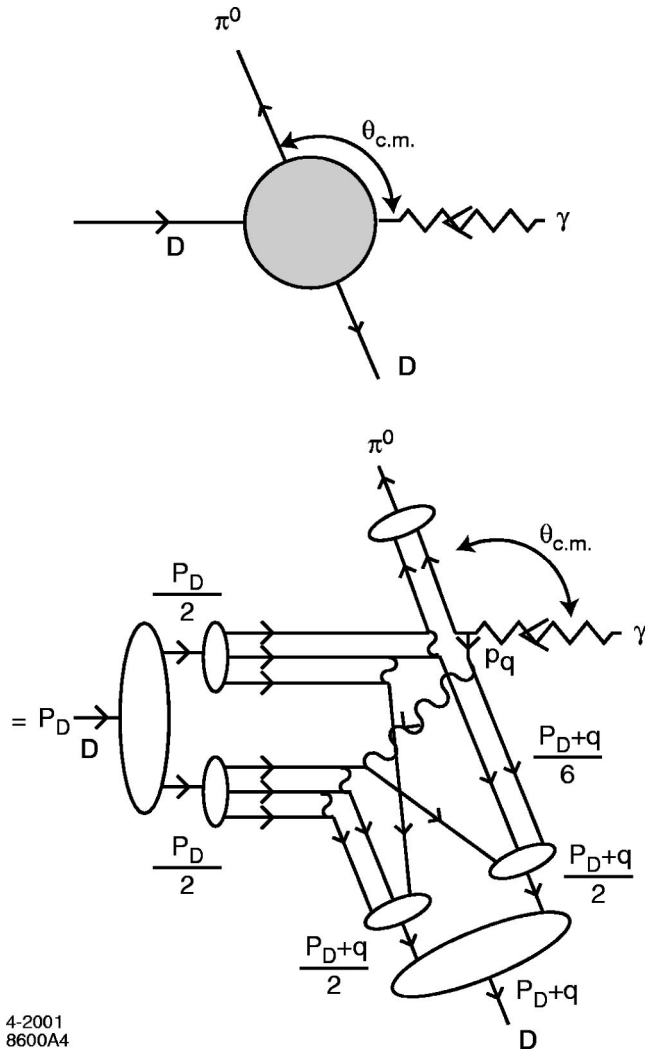

FIG. 4. Illustration of the basic QCD mechanism in which the nuclear amplitude for $\gamma D \to \pi^0 D$ factorizes as a product of two on-shell nucleon amplitudes. The quark interchange allows the amplitude to proceed when the deuteron wave function contains only color-singlet clusters.

Recently, JLAB experimental data [14] on π^0 photoproduction from a deuteron target, up to a photon lab energy $E_{\rm lab}=4$ GeV, were presented as an example inconsistent with both constituent-counting rules (CCR) [7] and RNA [13] predictions. While the data at $\theta_{\rm c.m.}=136°$ are consistent with the CCR, predicted as s^{-13} scaling for the differential cross section $d\sigma/dt$, the data at $\theta_{\rm c.m.}=90°$ exhibit a large disagreement with this prediction. Also, the data at both angles were interpreted [14] as being inconsistent with the RNA approach. This is in sharp contrast to the recent measurements of the deuteron electric form factor $A(Q^2)$, which are consistent with both the CCR and RNA predictions in a similar four-momentum transfer range 2 GeV$^2 \leqslant Q^2 \leqslant$ 6 GeV^2 [6].

One potential explanation for this disagreement is odderon exchange [15]. Because the odderon has zero isospin and is odd under charge conjugation, such an exchange is allowed in the t channel of π^0 photoproduction. However, we shall show that the improved factorization given by Eqs. (4) and (5) is in reasonably good agreement with the recent JLAB data [14] for $\gamma D \to \pi^0 D$ and the available $\gamma p \to \pi^0 p$ data [16–20] as well as the existing $eD \to eD$ and $ep \to ep$ data. There is thus no need to invoke any additional anomalous contribution to understand the new data [14].

We will also predict results for $\gamma D \to \pi^0 D$ at energies not yet attained. Furthermore, we will analyze the π^0 transverse momentum P_T dependence of the amplitude $\mathcal{M}_{\gamma D \to \pi^0 D}$ in the c.m. frame and find that the scaling of the predicted $\mathcal{M}_{\gamma D \to \pi^0 D}$ is not inconsistent with the CCR prediction of P_T^{-11} when the photon lab energy is only a few GeV for both values of $\theta_{\rm c.m.}$, 90° and 136°.

In the following section, Sec. II, we first briefly summarize the kinematics involved in the π^0 photoproduction process and then present a derivation of the improved factorization given by Eqs. (4) and (5). In Sec. III, we show the numerical results for $\mathcal{M}_{\gamma D \to \pi^0 D}$ as predicted by the factorization and compare the results with the recent JLAB data [14]. We also analyze the P_T dependence of $\mathcal{M}_{\gamma D \to \pi^0 D}$ as a

function of $E_{\rm lab}$ for $\theta_{\rm c.m.}=90°$ and 136°. Our conclusions and some discussion follow in Sec. IV.

II. KINEMATICS AND FACTORIZATION

A. π^0 Photoproduction kinematics

The Mandelstam [21] variables of the $\gamma D\to\pi^0 D$ process are given by

$$s=(q_\gamma+p_D)^2,\quad t=(q_\gamma-q_\pi)^2,\quad u=(p_D-q_\pi)^2, \quad (7)$$

where $p_D=\Sigma_{a=1}^{6}p_a$ is the momentum of the target deuteron and q_γ, q_π, and p_a are the momenta of the photon, pion, and ath quark of the deuteron. In the γ-D c.m. frame, where experimental results are reported, these variables are related to the photon energy and pion momentum by

$$\begin{aligned} s&=[E_\gamma^{\rm c.m.}+\sqrt{m_D^2+(E_\gamma^{\rm c.m.})^2}]^2,\\ t&=m_\pi^2-2E_\gamma^{\rm c.m.}[\sqrt{m_\pi^2+(\boldsymbol{q}_\pi^{\rm c.m.})^2}-|\boldsymbol{q}_\pi^{\rm c.m.}|\cos\theta_{\rm c.m.}], \quad (8)\\ u&=m_D^2+m_\pi^2-2[\sqrt{m_D^2+(\boldsymbol{q}_\pi^{\rm c.m.})^2}\sqrt{m_\pi^2+(\boldsymbol{q}_\pi^{\rm c.m.})^2}\\ &\quad+E_\gamma^{\rm c.m.}|\boldsymbol{q}_\pi^{\rm c.m.}|\cos\theta_{\rm c.m.}], \end{aligned}$$

with m_D the deuteron mass and $\theta_{\rm c.m.}$ the angle between the photon and the π^0 in the c.m. frame. Here, also in the c.m. frame, the photon energy and the magnitude of π^0 momentum are given by $E_\gamma^{\rm c.m.}=(s-m_D^2)/2\sqrt{s}$ and $|\boldsymbol{q}_\pi^{\rm c.m.}|=\sqrt{(s+m_\pi^2-m_D^2)^2/4s-m_\pi^2}$, respectively. The transverse momentum of the π^0 is then given by $P_T=|\boldsymbol{q}_\pi^{\rm c.m.}|\sin\theta_{\rm c.m.}$ and, if all the masses are neglected $P_T\approx\sqrt{tu/s}$. This simple expression is written to provide qualitative guidance to the reader. Our numerical calculations use the correctly computed value of P_T.

The Mandelstam variables s_N, t_N, and u_N of the process $\gamma N\to\pi^0 N$ can also be defined, with the deuteron momentum in Eq. (7) replaced by the nucleon momentum $p_N=\Sigma_{a=1}^{3}p_a$. In the γ-N c.m. frame of the $\gamma N\to\pi^0 N$ process, the photon energy and the magnitude of the π^0 momentum are given by $(E_\gamma^{\rm c.m.})_N=(s_N-m_N^2)/2\sqrt{s_N}$ and $(\boldsymbol{q}_\pi^{\rm c.m.})_N=\sqrt{(s_N+m_\pi^2-m_N^2)^2/4s_N-m_\pi^2}$, respectively, with the nucleon mass being m_N.

One can find the magnitude of the invariant amplitude $\mathcal{M}_{\gamma D\to\pi^0 D}(u,t)$ from the experimental differential cross section data by using

$$|\mathcal{M}_{\gamma D\to\pi^0 D}(u,t)|=4(s-m_D^2)\sqrt{\pi\frac{d\sigma}{dt}(\gamma D\to\pi^0 D)}. \quad (9)$$

Similarly, we obtain the invariant amplitude $|\mathcal{M}_{\gamma N\to\pi^0 N}(u_N,t_N)|$ from the available data for $\gamma p\to\pi^0 p$ [16–20]. The proton data and the factorization formula (4) can then be used to predict $|\mathcal{M}_{\gamma D\to\pi^0 D}(u,t)|$. We take the generic nucleon form factor $F_N(t)$ to be $[1-t/(0.71\ {\rm GeV}^2)]^{-2}$ and the reduced deuteron form factor [22] $f_d(t)\approx 2.14/[1-t/(0.28\ {\rm GeV}^2)]$, as determined by the analyses of the elastic deuteron form factors [23]. As one can see in the previous analysis [5], the experimental data for $|t|\leqslant 2\ {\rm GeV}^2$ are better described without the logarithmic corrections. The normalization constant C' in Eq. (4) is then fixed by the largest $E_{\rm lab}$ data point of $\gamma D\to\pi^0 D$ amplitude [14] at $\theta_{\rm c.m.}=90°$ and is obtained as $C'\approx 0.8$.

B. New improved RNA factorization

The factorization given by Eq. (4) can be derived in analogy with earlier work on the deuteron form factor [12]. The first step is to replace at the quark level the electromagnetic vertex $\gamma q\to q$ with a photoproduction amplitude $\gamma q\to\pi^0 q$. Let $\mathcal{M}_{\gamma q\to\pi^0 q}(q_\gamma,q_\pi,p_a)$ be the amplitude for this subprocess, with q_γ, q_π, and p_a the momenta of the photon, pion, and ath quark, respectively. The full amplitude for the hadronic process $\gamma D\to\pi^0 D$ can be transcribed from Eq. (2.10) of [12], with insertion of $\mathcal{M}_{\gamma q\to\pi^0 q}$, as

$$\begin{aligned} &\mathcal{M}_{\gamma D\to\pi^0 D}(u,t)\\ &\quad=\sum_{a=1}^{6}\int[dx]_i[d^2k_\perp]_i\Psi_D^*(x_i,\boldsymbol{k}_{\perp i}+(\delta_{ia}-x_i)\boldsymbol{q}_\perp)\\ &\qquad\times\mathcal{M}_{\gamma q\to\pi^0 q}(q_\gamma,q_\pi,p_a)\Psi_D(x_i,\boldsymbol{k}_{\perp i}) \quad (10)\end{aligned}$$

where Ψ_D is the valence wave function, $q\equiv q_\gamma-q_\pi$ is the momentum transfer, and

$$\begin{aligned}[dx]_i&=\delta\left(1-\sum_{i=1}^{6}x_i\right)\prod_{i=1}^{6}\frac{dx_i}{x_i},\\ [d^2k_\perp]_i&=16\pi^3\delta^2\left(\sum_{i=1}^{6}\boldsymbol{k}_{\perp i}\right)\prod_{i=1}^{6}\frac{d^2k_{\perp i}}{16\pi^3}. \quad (11)\end{aligned}$$

The reference frame has been chosen such that $q^+\equiv q^0+q^3=0$.

The deuteron wave function factorizes in the manner described by Eq. (2.23) of [12], which reads

$$\begin{aligned} &\sum_{a=1}^{6}\Psi_D^*(x_i,\boldsymbol{k}_{\perp i}+(\delta_{ia}-x_i)\boldsymbol{q}_\perp)\\ &\quad=\left[\sum_{a=1}^{3}\sum_{b=4}^{6}+\sum_{a=4}^{6}\sum_{b=1}^{3}\right]\frac{x_a}{1-x_a}\frac{1}{q_\perp^2}\\ &\qquad\times V(x_i,(\delta_{ia}-x_i)\boldsymbol{q}_\perp;x_j,[y\delta_{ja}+(1-y)\delta_{jb}-x_j]\boldsymbol{q}_\perp)\\ &\qquad\times\psi_N(z_i,\boldsymbol{k}'_{\perp i}+(\delta_{ia}-z_i)y\boldsymbol{q}_\perp)\\ &\qquad\times\psi_N(z_j,\boldsymbol{k}'_{\perp j}+(\delta_{jb}-z_j)(1-y)\boldsymbol{q}_\perp)\psi^d(0), \quad (12)\end{aligned}$$

where $\psi^d(0)$ is the body wave function of the deuteron at the origin and

$$\begin{aligned} &y=\sum_{i=1}^{3}x_i,\quad \boldsymbol{l}_\perp=\sum_{i=1}^{3}\boldsymbol{k}_{\perp i},\quad z_i=\frac{x_i}{y},\quad \boldsymbol{k}'_{\perp i}=\boldsymbol{k}_{\perp i}-z_i\boldsymbol{l}_\perp,\\ &z_j=\frac{x_j}{1-y},\quad \boldsymbol{k}'_{\perp j}=\boldsymbol{k}_{\perp j}+z_j\boldsymbol{l}_\perp. \quad (13)\end{aligned}$$

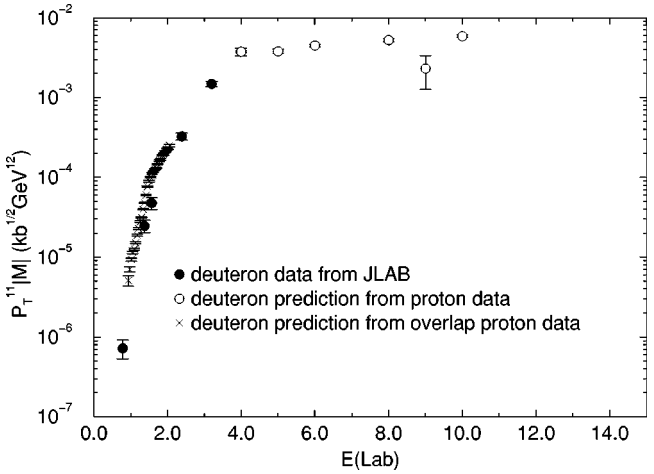

FIG. 5. $P_T^{11}|\mathcal{M}_{\gamma D\to\pi^0 D}|$ vs photon lab energy $E_{\rm lab}$ at $\theta_{\rm c.m.}=90°$. The filled circles are obtained directly from the recent JLAB $\gamma D\to\pi^0 D$ data [14], and the crosses and open circles are our predictions from the $\gamma p\to\pi^0 p$ data presented in Ref. [16–18]. Note that an open circle is overlaid on top of a filled circle for the overlapping data point at $E_{\rm lab}=4$ GeV.

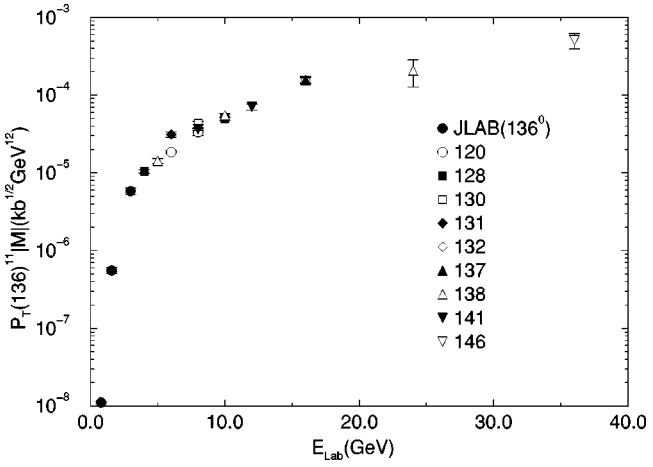

FIG. 6. $P_T^{11}(136)|\mathcal{M}_{\gamma D\to\pi^0 D}|$ vs photon lab energy $E_{\rm lab}$ with $P_T^{11}(136)$ defined by the P_T value computed at $\theta_{\rm c.m.}=136°$. This definition is due to the fact that the $\theta_{\rm c.m.}$ values of the $\gamma p\to\pi^0 p$ data are near 136° but not exactly equal. The filled circles are obtained directly from the recent JLAB $\gamma D\to\pi^0 D$ data [14], and the other symbols are our predictions based on $\gamma p\to\pi^0 p$ data at angles near $\theta_{\rm c.m.}=136°$, presented in Refs. [16–18].

In the weak binding limit, the value of y is approximately 1/2, $\boldsymbol{l}_\perp$ is approximately zero, and the kernel V contributes only a constant. The deuteron amplitude (10) reduces to the analog of Eq. (2.24) in Ref. [12]

$$\begin{aligned}\mathcal{M}_{\gamma D\to\pi^0 D}(u,t)&=\frac{C}{q_\perp^2}|\psi^d(0)|^2\Bigg\{\sum_{a=1}^{3}\int[dz]_i[d^2k'_\perp]_i\\&\times\psi_N^*\left(z_i,\boldsymbol{k}'_{\perp i}+(\delta_{ia}-z_i)\frac{\boldsymbol{q}_\perp}{2}\right)\\&\times\mathcal{M}_{\gamma q\to\pi^0 q}(q_\gamma,q_\pi,p_a)\psi_N(z_i,\boldsymbol{k}'_{\perp i})\\&\times\sum_{b=4}^{6}\int[dz]_j[d^2k'_\perp]_j\psi_N^*\left(z_j,\boldsymbol{k}'_{\perp j}+(\delta_{jb}-z_j)\frac{\boldsymbol{q}_\perp}{2}\right)\\&\times\psi_N(z_j,\boldsymbol{k}'_{\perp j})+(a\leftrightarrow b)\Bigg\}.\end{aligned}\tag{14}$$

This result does not quite factorize because the quark amplitude $\mathcal{M}_{\gamma q\to\pi^0 q}$ depends on the full q_γ and q_π, whereas the individual nucleons experience momentum transfers of $(q_\gamma-q_\pi)/2$. To relate this quark amplitude to the one for a subprocess involving only a nucleon, we use the spin-averaged form of the amplitude obtained by Carlson and Wakely [24]

$$|\mathcal{M}_{\gamma q\to\pi^0 q}(\hat u,\hat t)|^2\sim\hat t\frac{\hat s^2+\hat u^2}{\hat s^2\hat u^2},\tag{15}$$

where $\hat s=(q_\gamma+p_a)^2$, $\hat t=(q_\gamma-q_\pi)^2=t$, and $\hat u=(p_a-q_\pi)^2$. For photoproduction from a single nucleon, embedded in the deuteron, we have instead the quark-level invariants

$$\hat s_N=(q_\gamma/2+p_a)^2,$$

$$\hat t_N=(q_\gamma/2-q_\pi/2)^2=\hat t/4,\quad \hat u_N=(p_a-q_\pi/2)^2.\tag{16}$$

The quark momentum is the same in both cases, simply because it is the same quark. In the zero-mass limit we have $\hat s_N=\hat s/2$ and $\hat u_N=\hat u/2$. This [with Eq. (15)] leaves $|\mathcal{M}_{\gamma q\to\pi^0 q}(\hat u,\hat t)|^2\simeq|\mathcal{M}_{\gamma q\to\pi^0 q}(\hat u_N,\hat t_N)|^2$. Furthermore, the above values of $\hat s_N,\hat t_N,\hat u_N$ correspond to using $q_\gamma/2$ and $q_\pi/2$ in evaluating the proton photoproduction amplitude. With these values the factorization can now be completed to obtain Eq. (4). A similar derivation can be constructed for a relation between the amplitudes of $eD\to eD$ and $eN\to eN$ processes, from which one can prove Eq. (5). The corrections to these factorization formulas are generally expected to be of order $1/P_T^2$. The computation of these terms is beyond the scope of this paper.

III. COMPARISON WITH EXPERIMENT

From the recent JLAB $\gamma D\to\pi^0 D$ data [14], we computed the corresponding invariant amplitudes using Eq. (9) both for $\theta_{\rm c.m.}=90°$ and 136°. We then used our factorization formula Eq. (4) to predict $|\mathcal{M}_{\gamma D\to\pi^0 D}|$ with input from the available $\gamma p\to\pi^0 p$ data [16–20]. The results are presented in Figs. 5 and 6. There are no data for pion production from a neutron target, and we assume here that the proton and neutron amplitudes have the same dependence on u and t. This assumption is reasonable for the production of neutral pions, which contain u and d quarks with equal probability and therefore couple to the proton and neutron in similar ways. We do not consider charged pion production.

In Fig. 5, the normalization of our prediction is fixed (at $C'=0.8$) by the overlapping data point at $E_{\rm lab}=4$ GeV,

which is the highest photon lab energy used in the JLAB $\gamma D \to \pi^0 D$ experiment [14]. It is interesting to find that the general trend of our prediction (the open circles) is very similar to that of the direct result from the JLAB data [14], shown as filled circles. The prediction is remarkably consistent with the CCR prediction. In addition, our ''prediction'' in the $E_{\rm lab}$ overlap region, denoted by crosses, mimics the shape of the direct result. The crosses are systematically above all the filled circles by 50% or more (on a linear scale). This difference could be absorbed into the determination of the normalization; however, the factorization is expected to be less accurate at these lower energies. We note that the virtuality of the struck-quark propagator discussed in Sec. I (see also Figs. 3 and 4) is approximately given by $|t|/3 \approx 2$ GeV^2 for $E_{\rm lab}=4$ GeV, which satisfies the condition mentioned in the Introduction. We, therefore, fix the normalization C' of our factorization formula Eq. (4) from the data at the highest available photon lab energy, i.e., $E_{\rm lab}=4$ GeV. We expect non-negligible corrections to our formula at all energies we consider here, but these are expected to become increasingly small, falling off as P_T^{-2}, as the energy increases. Also, one should note that there is a resonance contribution in the $\gamma p \to \pi^0 p$ data [16], in the region of 700 MeV $\leqslant E_{\rm lab} \leqslant$ 800 MeV, which could bias a normalization done at lower energies.

In obtaining Fig. 6, we use input from the proton data [16–20] in the vicinity of $\theta_{\rm c.m.}=136°$ to compute the scattering amplitude for a deuteron target. We were unable to find $\gamma p \to \pi^0 p$ data exactly at $\theta_{\rm c.m.}=136°$ in the $E_{\rm lab}$ energy range considered here. Using the same procedure for determining the normalization as in obtaining Fig. 5, we find that our prediction is nicely connected to the direct calculation from the JLAB data [14], again shown as filled circles. The prefactor P_T^{11} is computed at $\theta_{\rm c.m.}=136°$ for all data points. The scaling behavior predicted by perturbative QCD, $P_T^{11}|\mathcal{M}_{\gamma D \to \pi^0 D}| \sim$ const at fixed $\theta_{\rm c.m.}$, does not appear to work as well at $\theta_{\rm c.m.}=136°$ in Fig. 6 in comparison with the $\theta_{\rm c.m.}=90°$ data shown in Fig. 5. This is in part due to the fact that the high power of 11 makes the prefactor P_T^{11} very sensitive to the variation in the values of $\theta_{\rm c.m.}$. The accuracy of the present calculations is, therefore, limited by the lack of data for both the deuteron and proton target at the same fixed values of θ, and more $\gamma D \to \pi^0 D$ and $\gamma p \to \pi^0 p$ data are needed. However, if we look only at the data points that are close to $\theta_{\rm c.m.}=136°$, such as the filled triangles at 137° and open triangles at 138°, and take experimental errors into account, CCR scaling is not inconsistent for $E_{\rm lab}$ above 10 GeV.

IV. CONCLUSIONS AND DISCUSSION

We have analyzed the predictions of perturbative QCD for coherent photoproduction on the deuteron $\gamma D \to \pi^0 D$ at large momentum transfer using a new form of reduced amplitude factorization displayed in Eq. (4). The underlying principle of the analysis is the cluster decomposition theorem for the deuteron wave function at small binding: the nuclear coherent process can proceed only if each nucleon absorbs an equal fraction of the overall momentum transfer. Furthermore, each nucleon must scatter while remaining close to its mass shell. Thus the nuclear photoproduction amplitude $\mathcal{M}_{\gamma D \to \pi^0 D}(u,t)$ factorizes as a product of three factors: (1) the nucleon photoproduction amplitude $\mathcal{M}_{\gamma N_1 \to \pi^0 N_1}(u/4,t/4)$ at half of the overall momentum transfer and at the same overall center of mass angle, (2) a nucleon form factor $F_{N_2}(t/4)$ at half the overall momentum transfer, and (3) the reduced deuteron form factor $f_d(t)$, which according to perturbative QCD, has the same monopole falloff as a meson form factor. The on-shell condition requires the center-of-mass angle of pion photoproduction on the nucleon N_1 to be commensurate with the center-of-mass angle of pion photoproduction on the deuteron. The reduced amplitude prediction is consistent with the constituent counting rule $p_T^{11}\mathcal{M}_{\gamma D \to \pi^0 D} \to F(\theta_{\rm c.m.})$ at large momentum transfer. A comparison with the recent JLAB data for $\gamma D \to \pi^0 D$ of Meekins *et al.* [14] and the available $\gamma p \to \pi^0 p$ data [16–20] shows good qualitative agreement between the perturbative QCD prediction and experiment over a large range of momentum transfers and center-of-mass angles. It would be useful to confirm or deny this agreement with further measurements on both proton and deuteron targets. However, there are additional uncertainties due to the lack of knowledge about pion production from the neutron.

We have also used reduced amplitude scaling for the elastic electron-deuteron scattering to show

$$\frac{\mathcal{M}_{\gamma D \to \pi^0 D}}{\mathcal{M}_{eD \to eD}} = C' \frac{\mathcal{M}_{\gamma p \to \pi^0 p}}{\mathcal{M}_{ep \to ep}}. \tag{17}$$

This scaling is also consistent with the experiment. The constant C' is found to be close to 1, suggesting similar underlying hard-scattering contributions. No anomalous contributions, such as might derive from odderon exchange are required.

ACKNOWLEDGMENTS

This work was supported in part by the Department of Energy, Contract Nos. DE-AC03-76SF00515 (S.J.B.), DE-FG02-98ER41087 (J.R.H.), DE-FG02-96ER40947 (C.-R.J.), and DE-FG03-97ER4104 (G.A.M.).

[1] S.J. Brodsky, H.-C. Pauli, and S.S. Pinsky, Phys. Rep. **301**, 299 (1998).
[2] C.-R. Ji and S.J. Brodsky, Phys. Rev. D **34**, 1460 (1986).
[3] S.D. Drell and T.M. Yan, Phys. Rev. Lett. **24**, 181 (1970).
[4] G. West, Phys. Rev. Lett. **24**, 855 (1970).
[5] S.J. Brodsky, C.-R. Ji, and G.P. Lepage, Phys. Rev. Lett. **51**, 83 (1983).
[6] L.C. Alexa *et al.*, Phys. Rev. Lett. **82**, 1374 (1999).
[7] S.J. Brodsky and G.R. Farrar, Phys. Rev. Lett. **31**, 1153 (1973); Phys. Rev. D **11**, 1309 (1975); V.A. Matveev, R.M. Muradyan, and A.V. Tavkhelidze, Lett. Nuovo Cimento Soc. Ital. Fis. **7**, 719 (1973).
[8] J. Napolitano *et al.*, Phys. Rev. Lett. **61**, 2530 (1988); S.J. Freedman *et al.*, Phys. Rev. C **48**, 1864 (1993).
[9] J.E. Belz *et al.*, Phys. Rev. Lett. **74**, 646 (1995).
[10] C.W. Bochna *et al.*, Phys. Rev. Lett. **81**, 4576 (1998).
[11] J.M. Namyslowski, Report No. IFT/80/3-WARSAW, 1980 (unpublished).
[12] S.J. Brodsky and C.-R. Ji, Phys. Rev. D **33**, 2653 (1986).
[13] S.J. Brodsky and J.R. Hiller, Phys. Rev. C **28**, 475 (1983); **30**, 412(E) (1984).
[14] D.G. Meekins *et al.*, Phys. Rev. C **60**, 052201 (1999).
[15] I.F. Ginzburg, D.Yu. Ivanov, and V.G. Serbo, Yad. Fiz. **56**, 45 (1993) [Phys. At. Nucl. **56**, 1474 (1993)]; E.R. Berger and O. Nachtmann, Nucl. Phys. (Proc. Suppl.) **79A**, 352 (1999).
[16] A. Imanishi *et al.*, Phys. Rev. Lett. **54**, 2497 (1985).
[17] M.A. Shupe *et al.*, Phys. Rev. Lett. **40**, 271 (1978).
[18] G.C. Bolon *et al.*, Phys. Rev. Lett. **18**, 926 (1967).
[19] R.L. Anderson *et al.*, Phys. Rev. Lett. **30**, 627 (1973).
[20] R.L. Anderson *et al.*, Phys. Rev. Lett. **26**, 30 (1971).
[21] S. Mandelstam, Phys. Rev. **112**, 1344 (1958).
[22] S.J. Brodsky and B.T. Chertok, Phys. Rev. Lett. **37**, 269 (1976); Phys. Rev. D **14**, 3003 (1976).
[23] R.G. Arnold *et al.*, Phys. Rev. Lett. **35**, 776 (1975).
[24] C.E. Carlson and A.B. Wakely, Phys. Rev. D **48**, 2000 (1993).